Thermophysics and Aeromechanics, *2015*, *Vol. 22*, *No. 5*

Direct numerical simulation of transition to turbulence in a supersonic boundary layer*

A.N. Kudryavtsev and D.V. Khotyanovsky

Khristianovich Institute of Theoretical and Applied Mechanics SB RAS, *Novosibirsk*, *Russia*

E-mail: khotyanovsky@itam.nsc.ru

(*Received March 25*, *2015*)

Based on full unsteady compressible Navier–Stokes equations a direct numerical simulation of the linear and nonlinear stages of the laminar-turbulent transition in boundary layer of a flate plate at the freestream Mach number M = 2 is carried out.

Key words: direct numerical simulation, laminar-turbulent transition, supersonic boundary layer.

Introduction

The transition to turbulence in a boundary layer leads to a substantial increase in the drag force acting on the streamlined body. Therefore, the elucidation of the mechanisms of the boundary layer tripping and especially the search for possible techniques of transition control is an important scientific problem whose solution would enable one to substantially increase the economy of the existing vehicles and help in the development of new vehicles. In particular, the development of a new generation of supersonic air liners requires a good understanding of the main peculiarities of the transition to turbulence in supersonic boundary layer, especially in cruise regime, that is at the freestream Mach numbers close to M = 2.

It is well known from the results of the linear theory of the boundary layer stability [1, 2] that at moderate supersonic speeds, the flow is unstable only to one mode of disturbances. The disturbances of this so-called first mode are the vortex disturbances similar to the Tollmien–Schlichting waves in the incompressible boundary layer. Both in subsonic boundary layers and at high Mach numbers ($M \geq 4$), the two-dimensional waves are the most unstable (in the latter case, these are the acoustic disturbances of the second mode). At moderate supersonic speeds, the amplification coefficient is maximum for three-dimensional disturbances propagating at a rather high angle of attack (50–70°) to the flow.

The results of linear theory have been confirmed experimentally. Experimental investigations of the development of disturbances in boundary layers have been started sufficiently long ago [3], but such investigations were conducted in especial detail in the works done during the last 25 years at the ITAM SB RAS (see, in particular, the works [4–6]).

* The work was financially supported by the Russian National Foundation (Grant No. 14-11-00490).

With the advent of powerful computers, there has appeared a possibility of a direct numerical simulation of nonlinear stages of the development of disturbances, which precede the transition, and the transition process itself. In some of the first studies of such a kind [7–8], the nonlinear interaction of disturbances and the transition were investigated under the assumption on the flow periodicity along the streamwise coordinate so that the instability developed in time. The direct numerical simulation was carried out later in a more realistic spatial formulation — for the Mach number range under consideration, the most detailed computations were done in recent works [9–10].

Unfortunately, there are in the domestic literature practically no works on the direct numerical simulation of the instability development and the transition to turbulence at supersonic speeds. The series of the works [11–13] devoted to the receptivity and early stages of the development of two-dimensional disturbances in hypersonic boundary layer is an important exception.

Despite sufficiently intense experimental and numerical investigations there is no complete understanding of the mechanisms controlling the transition to turbulence in boundary layer at moderate supersonic speeds. It appears that two transition scenarios are possible. One of them is based on the resonance interaction of the inclined fundamental wave (having the frequency ω_m corresponding to the maximum amplification factor) and two waves, which also propagate at an incidence to the flow and which are its subharmonics (that is the waves with frequency $\omega_m/2$). At a frequency dependence of the wave vector components $\omega = \omega(\alpha, \beta)$, which is known from the linear theory, the angles of the propagation of subharmonics with respect to the main stream can be determined from the requirements of the satisfaction of the phase synchronization conditions. Such an asymmetric subharmonic resonance was revealed experimentally [5]. Another possible scenario of transition termed the "oblique breakdown" in the English-language literature was proposed in the work [14] on the basis of a direct numerical simulation of the development of disturbances in sub- and supersonic (M = 1.6) boundary layers, which was done therein. It consists of a nonlinear interaction of two fundamental waves propagating at the angles $\pm\chi$ to the flow. These waves form a resonance wave triad with a stationary vortex disturbance. Such a mechanism possesses a lower threshold amplitude for the onset of the nonlinear interaction of waves and must lead to a more rapid transition. As follows from a thorough comparison of computed data with experimental results, which was done in the work [15], the resonance of inclined waves with a steady wave disturbance may be identified among the results presented in [5], so that this work may be considered as a direct experimental confirmation of the existence of such a mechanisms.

In the present work, a direct numerical simulation of the linear and nonlinear stages of the spatial interaction of growing disturbances and the initial stages of the laminar-turbulent transition in the boundary layer on a flat plate at the freestream Mach number M = 2 is carried out on the basis of the full unsteady Navier–Stokes equations of compressible gas.

1. Problem statement

The problem of the development of an unstable boundary layer on a flat plate streamlined by a supersonic air flow at a zero angle of attack with the Mach number M = 2 is considered. The flow is described within the framework of the continuum model for a perfect compressible viscous heat-conducting gas with the adiabatic exponent $\gamma = 1.4$. The full three-dimensional Navier–Stokes equations are used as the mathematical model of the medium. The stress tensor is assumed to be linearly related to the tensor of deformation rates, the volumetric viscosity equals zero according to the Stokes hypothesis, and the Fourier law holds for thermal fluxes.

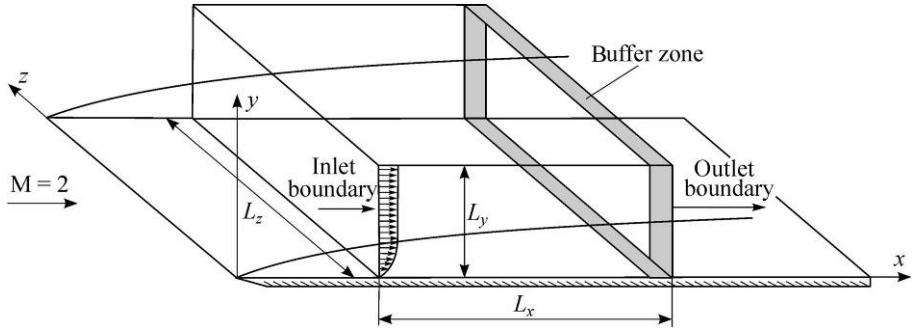

Fig. 1. Computational domain schematic.

The dynamic viscosity μ depends on temperature T according to the power law with exponent of 0.76. The Prandtl number Pr = 0.72. The flow scheme and the schematic of the computational domain are presented in Fig. 1. The origin of a Cartesian coordinate system lies on the sharp leading edge of the flat plate. The x-axis coincides with the direction of the velocity vector U of the supersonic free stream, the y-axis is directed along a normal to the plate, the z-axis coincides with the leading edge. The plate is assumed to have an infinite extension along the x- and z-coordinates. The computational domain has the shape of a parallelepiped whose lower face coincides with the plate plane $y = 0$. The domain sizes along the x-, y-, and z-coordinates are equal to L_x, L_y, and L_z, respectively. The lower face of the computational domain lies at the distance $x = x_0$ from the leading edge. The flow in boundary layer is assumed laminar and self-similar in the range of coordinates $0 < x < x_0$. If it is otherwise not mentioned, the Blasius thickness $\delta = \sqrt{\nu x / U}$ of the boundary layer in section $x = x_0$, which corresponds to the left inlet boundary of the computational domain $\delta_0 = \sqrt{\nu x_0 / U}$, where ν is the kinematic viscosity, is used as the reference length. The inlet boundary location was chosen at a sufficient distance from the plate leading edge to ensure that the boundary layer was unstable here. As the data of experiments [6] show, the corresponding conditions are reached at the Reynolds number determined in terms of the local thickness of the boundary layer, $\mathrm{Re}_\delta = U\delta/\nu = 500$. The corresponding Reynolds number determined in terms of the distance from the plate leading edge equals $\mathrm{Re}_x = Ux/\nu = \mathrm{Re}_\delta^2 = 250\,000$.

2. Numerical simulation technique

The modeling of the unstable boundary layer development and the transition to turbulence is based on a direct numerical solution of three-dimensional unsteady Navier–Stokes equations using the program package CFS3D developed at the Laboratory of the computational aerodynamics of ITAM SB RAS. The fifth-order finite-difference WENO (Weighted Essentially Non-Oscillatory) scheme [16] is used for the spatial discretization of convective terms. The diffusion terms of the Navier–Stokes equations are approximated with the aid of the fourth-order central-difference formulas on a compact stencil. The numerical algorithm is explicit, the fourth-order Runge–Kutta–Gill algorithm [17] is employed for the numerical solution integration in time. The time step is chosen automatically in the process of numerical computation from the condition that the generalized Courant–Friedrichs–Levy number (including also the stability condition for viscous terms) CFL = 0.75. The method of the numerical solution of the Navier–Stokes equations was discussed

in detail in the work [18]. The numerical algorithm has been parallelized by the method of the computational domain decomposition and employs the MPI (Message Passing Interface) data exchange between the neighboring subregions. The code parallel efficiency amounts to about 80 % at the use of 64 central processors of the computational cluster.

The strategy of the numerical simulation of the unstable boundary layer development consists of several stages. At the first stage, one performs the computation of the main laminar flow. Since the main flow is homogeneous along the transversal coordinate z, the computations are carried out in the two-dimensional statement in the plane $z = 0$. At the left boundary of the computational domain ($x = x_0$), one specifies the profiles of the streamwise and normal components of the velocity vector and temperature, which have been obtained from a self-similar solution for a compressible boundary layer in the section under consideration along x, and the freestream pressure. At the upper boundary ($y = L_y$) as well as at the outlet boundary ($x = x_0 + L_x$), the values of variables are extrapolated from the computational domain interior. On the plate surface ($y = 0$), one specifies the no-slip conditions — the zero normal derivative of the pressure. The ratio of the wall temperature T_w to the temperature at the external edge of the boundary layer T_e has been taken to be equal to $T_w / T_e = 1.676$, which corresponds to the case of the adiabatically isolated plate at the number M = 2. As the initial data one specifies in the entire region the self-similar solution for the corresponding sections along x. The main flow is computed by the pseudo-unsteady method. The computational domain size along the streamwise coordinate was specified to be fairly large — $L_x = 3000$, the size along the normal coordinate is $L_y = 100$. The computational grid was clustered along the normal coordinate in the boundary layer region. A rectangular structured grid with the number of cells $N_x = 1024$ and $N_y = 150$ along the streamwise and normal coordinates, respectively, was used in computations.

At the second stage, the computation of the spatial development of growing disturbances in the boundary layer is carried out using the solution of full three-dimensional Navier–Stokes equations. An unsteady disturbed field is set at the inlet boundary in the form of eigenfunctions of the linear stability problem with given wave parameters. The linear stability task is solved in the inlet section for the given self-similar profiles of the main flow. At the outlet boundary, one specifies the mild non-reflective boundary conditions, and to prevent the reflection of disturbances inside the computational region ahead of the outlet boundary one performs the relaminarization of disturbances in a special buffer region (sponge layer) [19]. The results of test computations point to a minimum disturbing action of the outlet boundary on the flow field inside the computational region. At the execution of three-dimensional computations, the periodic boundary conditions along the transversal direction are used, and the computational domain size along the z coordinate is set equal to the wavelength of the three-dimensional linear disturbance along this coordinate. The number of cells along the transversal coordinate amounted to $N_z = 64$, thus, the total number of cells in the three-dimensional computational domain amounted to 9.8 millions.

3. Numerical simulation results

Figure 2 shows the results of numerical computations of the laminar main flow in the boundary layer of a flat plate at the flow Mach number M = 2 and the Reynolds number defined in terms of the boundary layer thickness in the inlet section, $\mathrm{Re}_{\delta 0} = 500$. The symbols show the profiles of the streamwise velocity component and temperature in section $x/\delta_0 = 2000$. Solid lines show the corresponding profiles obtained from the self-similar solution of the laminar boundary layer equations. As is seen in Fig. 2, the results of numerical computations agree well with the self-similar profiles of the main flow.

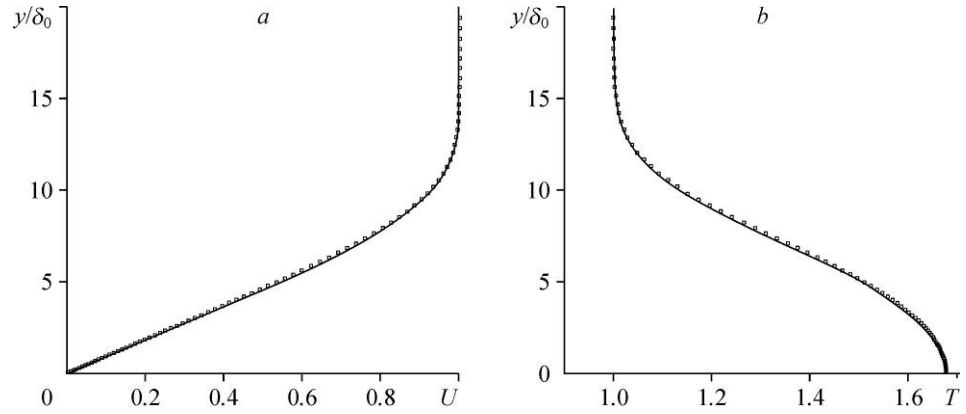

Fig. 2. Profiles of the streamwise velocity component (*a*) and temperature (*b*) of the main flow in comparison with the self-similar solution.

For the main flow, the investigation of the linear stability characteristics is carried out in the inlet section. Based on the numerical solution of the linear eigenvalue problem, the growing waves are sought, their wave characteristics and eigenfunctions are determined. As the conducted computations show, the most unstable disturbance of the boundary layer at the parameters under consideration is three-dimensional, with the inclination angle of the wave vector to the free-stream direction $\chi = 55°$ (Fig. 3). It is seen from the analysis of neutral curves in Fig. 3*a* that the main flow at $\mathrm{Re}_{\delta 0} = 500$, which corresponds to the inlet section, is unstable, and the increments of the disturbances growth with the angle $\chi = 55°$ exceed considerably the growth characteristics of two-dimensional disturbances. Figure 4 shows the results of the numerical simulation of the development of small-amplitude disturbances, for which one can neglect nonlinear effects. Solid curves correspond here to the exponential growth of the disturbance according to the linear theory. As is seen in the figure, the variation of the disturbance amplitude in streamwise direction in the initial interval ideally corresponds to the exponential growth with an increment predicted by the linear theory. The increment of the growth of the disturbance of a given frequency reduces downstream because of the alteration of the main flow characteristics (an increase in the local thickness of the boundary layer), and the flow finally stabilizes.

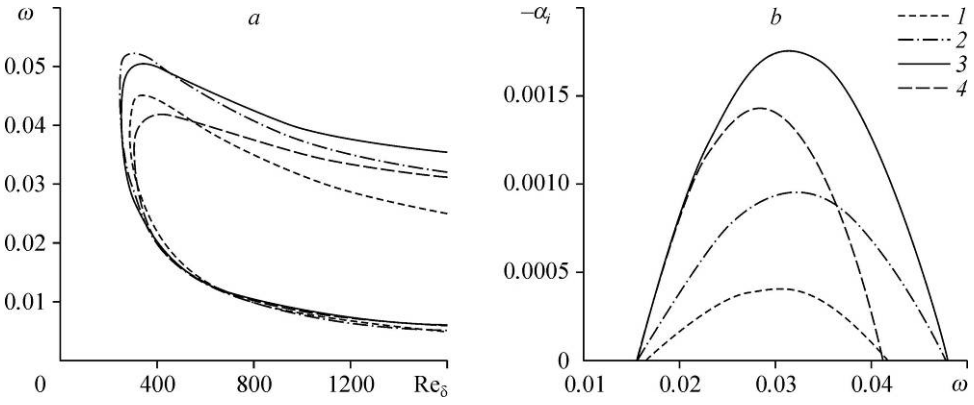

Fig. 3. Neutral stability curves at M = 2 (*a*) and the increments of the disturbances growth at M = 2, $\mathrm{Re}_{\delta} = 500$ (*b*) at different angles of the wave vector χ.

$\chi = 0°$ (*1*), 30° (*2*), 55° (*3*), 65° (*4*).

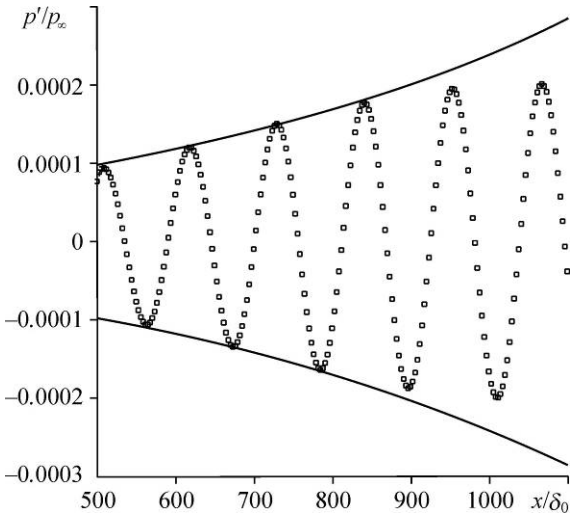

Fig. 4. Development of a small disturbance in a direct numerical simulation. Pressure fluctuations on the wall. Solid curves correspond to the exponential growth with the amplification increment according to the linear theory in section $x/\delta_0 = 500$.

At the investigation of a nonlinear development of disturbances at the inlet boundary, the three-dimensional instability waves were excited with frequencies corresponding to the maximum amplification coefficients of the linear theory. A superposition of two growing disturbances propagating at the angles $\chi = \pm 55°$ to the main stream direction was superimposed on the basic flow. The disturbance amplitude amounted, as a rule, to 0.5 % of the freestream velocity. The spatial development of such a disturbed field is shown in Fig. 5. At the development of disturbances with sufficiently high initial amplitudes, one observes in the flow the formation of a secondary flow in the form of streamwise vortex structures. Note that the formation of such streamwise vortices was observed previously in the computations of [19]. A typical size of the observed streamwise vortices has the order of the boundary layer thickness in the normal and transversal directions. At the simulation in a sufficiently long computational domain, one observes at very large distances along the streamwise coordinate the development of a secondary instability of the obtained flow with a rapid, bursting growth of three-dimensional fluctuations, which leads downstream to a laminar-turbulent transition. The instantaneous fields of gas-dynamic quantities acquire a high degree of chaotic character, which is well seen in Fig. 5.

Figure 6 shows the instantaneous flow fields in the (y, z) plane at different values of the x-coordinate. It is well seen that the streamwise structures forming in the boundary layer develop at the initial stage independently of each other. Their transverse size gradually increases downstream, and directly prior to the transition onset, the entire transverse flow field is entrained in the vortex motion.

The alteration of the velocity profiles of the mean flow is presented in Fig. 7 in different sections along the streamwise coordinate. The flow fields were averaged during a sufficiently long time interval, which was equal as a rule to eight periods of the instability wave. As is seen from the analysis of profiles in Fig. 7, the flow in boundary layer undergoes a transformation due to a nonlinear development of the disturbances from a purely laminar shape at the initial stage to the transitional shape characterized by a more filled velocity profile.

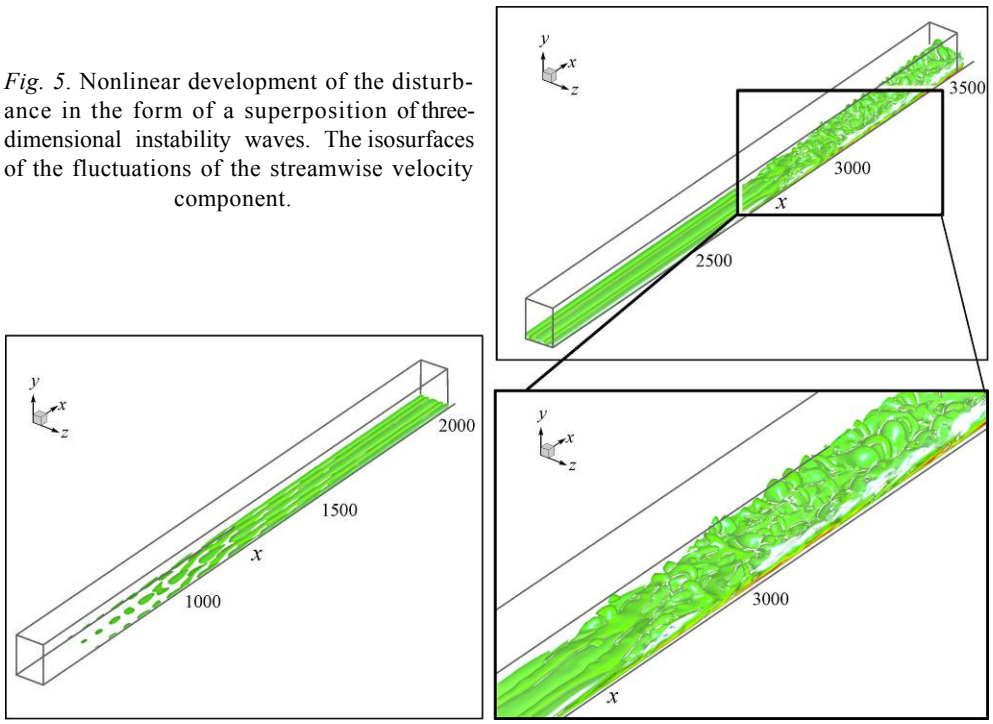

Fig. 5. Nonlinear development of the disturbance in the form of a superposition of three-dimensional instability waves. The isosurfaces of the fluctuations of the streamwise velocity component.

The distributions of the time-averaged skin-friction coefficient and the momentum thickness shown in Fig. 8 point to the fact that the onset of laminar-turbulent transition is followed by a considerable increase in these quantities.

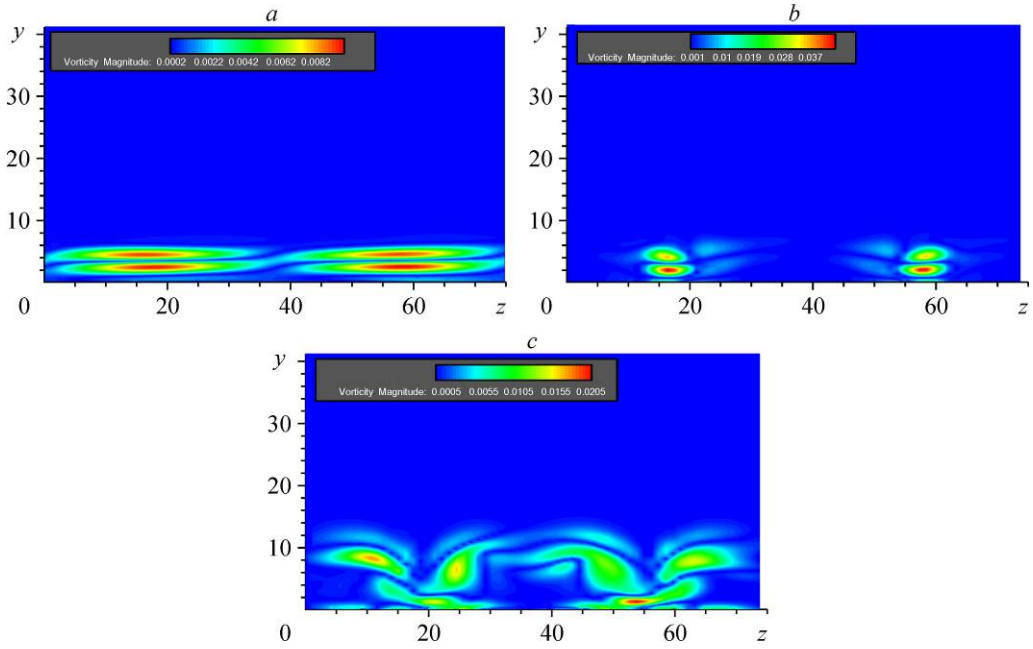

Fig. 6. Instantaneous field of the vorticity absolute value in cross sections. $x/\delta_0 = 1000$ (*a*), 2000 (*b*), 2600 (*c*).

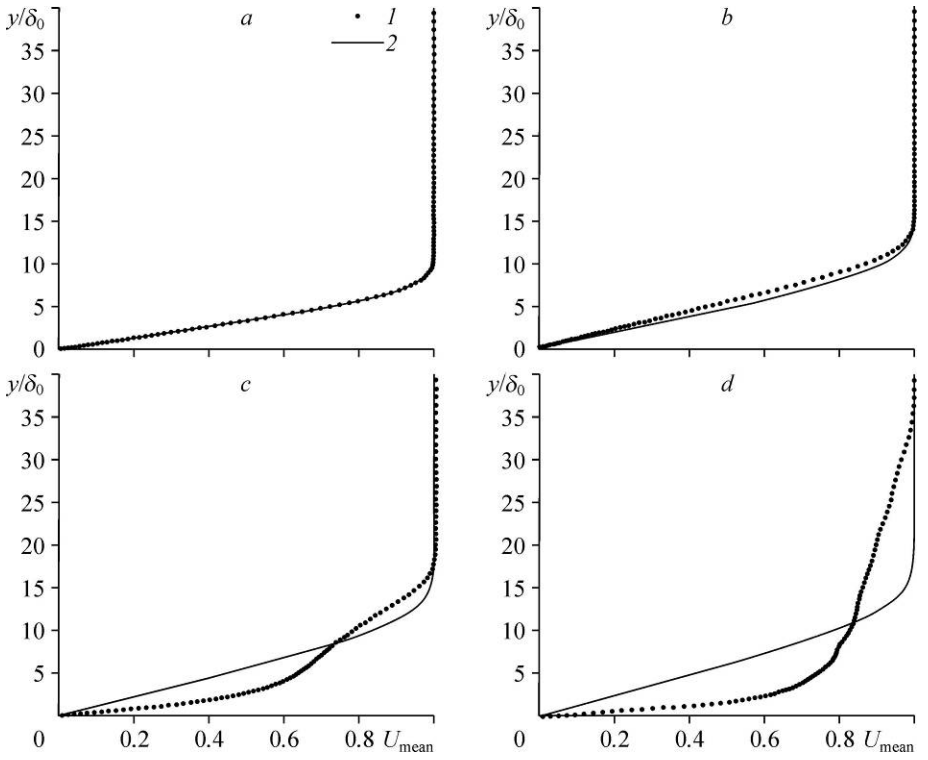

Fig. 7. Alteration of the velocity profile of mean flow in different sections as compared to the laminar self-similar solution.
1 — x/δ_0 = 1000 (*a*), 2000 (*b*), 2800 (*c*), 3400 (*d*);
2 — at laminar flow: x/δ_0 = 1000 (*1*), 2000 (*2*), 2800 (*3*), 3400 (*4*).

Figure 9 shows a comparison of the results of the present computation of the mean-square fluctuation of the mass flow rate in boundary layer with experimental data of [6]. As follows from the analysis of data, a direct numerical simulation enables a sufficiently good prediction of the qualitative form of the distribution of fluctuations along the streamwise coordinate as well as the obtaining of a good quantitative agreement with experiment in terms of the Reynolds number at the laminar-turbulent transition point. In particular, the presence of a local rise of the intensity of fluctuations of the mass flow rate in the computation and in experiments

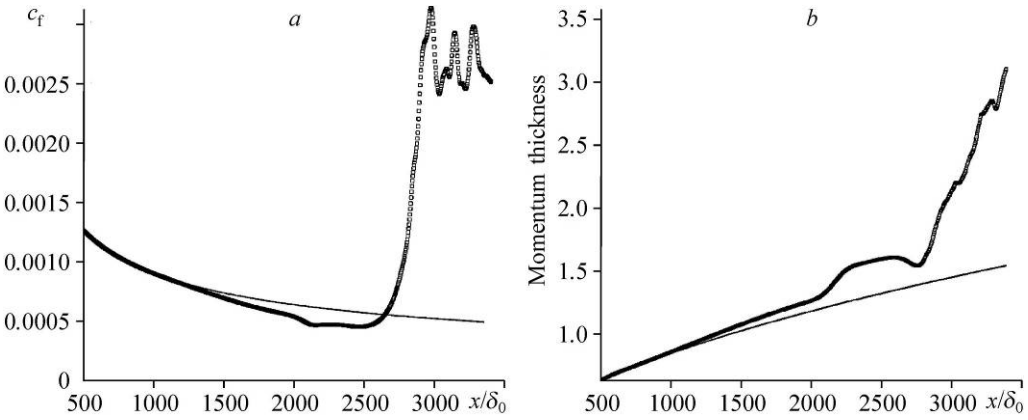

Fig. 8. Alteration of the skin-friction coefficient c_f (*a*) and the momentum thickness (*b*) along the plate.
Solid curves correspond to the laminar flow regime.

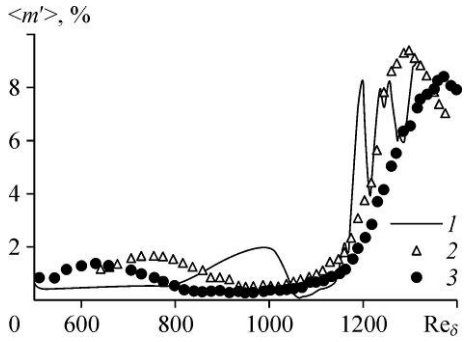

Fig. 9. Streamwise distribution of the mass flow rate fluctuations in the numerical simulation and in experiments of the work [6].
1 — present computation, *2* — experiment, artificial disturbances [6], *3* — experiment, natural disturbances [6].

calls attention. The location of the local maximum in computation corresponds to the value of the number $\mathrm{Re}_\delta \approx 1000$. In experiments, its value varies from $\mathrm{Re}_\delta \approx 630$ with natural disturbances up to $\mathrm{Re}_\delta \approx 760$ with artificial disturbances. The difference between the numerical and experimental data on the local maximum location is explained apparently by a difference in the disturbed state of the boundary layer in the computation and in experiment. The location of the laminar-turbulent transition onset corresponds to the Reynolds number $\mathrm{Re}_\delta \approx 1150$. It appears that it depends weakly on the technique of the excitation of the boundary layer instability, while being close in experiments of [6] to both the natural disturbances and the localized artificial disturbances as well as in computations with the excitation of the proper disturbances of the linear theory, which are periodic along z.

Conclusions

Based on the numerical solution of full unsteady Navier–Stokes equations a direct numerical simulation of linear and nonlinear stages of the development of growing three-dimensional disturbances and the onset of laminar-turbulent transition in boundary layer on a flat plate at the freestream Mach number M = 2 has been carried out. The stationary laminar base flow in the inlet section was excited by the most rapidly growing disturbances obtained from the solution of the linear problem of stability. These disturbances represent the three-dimensional Tollmien–Schlichting waves propagating at the angle $\chi = \pm 55°$ to the main flow direction. The numerical simulation data obtained at the computation of the main flow and the data on the growth of small disturbances in linear regime coincide well with the results of the boundary layer theory and the linear theory of hydrodynamic stability.

It has been found at the direct numerical simulation that the nonlinear development of three-dimensional disturbances leads at some downstream distance (at $\mathrm{Re}_\delta \approx 700$) to the formation of a slowly evolving streamwise vortex structures. Further one observes at about $\mathrm{Re}_\delta \approx 1150$ an abrupt growth of small-scale three-dimensional fluctuations, which leads to the laminar-turbulent transition. The transition onset is characterized by a substantial alteration of the velocity profiles of the averaged flow and by a sudden increase in skin friction and the boundary-layer thickness. The location of the laminar-turbulent transition onset agrees well with the experimental data of [6].

References

1. **L.M. Mack,** Boundary-layer stability theory, Doc. 90-277-REV-A (NASA CR 131501), 1969.
2. **S.A. Gaponov and A.A. Maslov,** Development of Disturbances in Compressible Flows, Nauka, Novosibirsk, 1980.
3. **J. Laufer and T. Vrebalovich,** Stability and transition of a supersonic laminar boundary layer on an insulated plate, J. Fluid Mech., 1960, Vol. 9, P. 257–299.
4. **A.D. Kosinov, A.A. Maslov, and S.G. Shevelkov,** Experiments on the stability of supersonic laminar boundary layers, J. Fluid Mech., 1990, Vol. 219, P. 621–633.
5. **A.D. Kosinov, N.V. Semionov, S.G. Shevelkov, and O.I. Zinin,** Experiments on instability of supersonic boundary layers, in: Nonlinear Instability of Nonparallel Flows. Springer, Berlin, Heidelberg, 1994, P. 196–205.

6. **Yu.G. Ermolaev, A.D. Kosinov, and N.V. Semionov,** Features of the weakly nonlinear interaction of instability waves in supersonic boundary layer, Vestnik NGU. Ser. Fizika, 2008, Vol. 3, No. 3, P. 3–13.
7. **N.D. Sandham and N.A. Adams,** Numerical simulation of boundary-layer transition at Mach two, Appl. Sci. Research, 1993, Vol. 51, P. 371–375.
8. **N.D. Sandham, N.A. Adams, and L. Kleiser,** Direct simulation of breakdown to turbulence following oblique instability waves in a supersonic boundary layer, Appl. Sci. Research, 1995, Vol. 54, P. 223–234.
9. **C.S.J. Mayer, S. Wernz, H.F. Fasel,** Numerical investigation of the nonlinear transition regime in a Mach 2 boundary layer , J. Fluid Mech., 2011, Vol. 668, P. 113–149.
10. **C.S.J. Mayer, D.A. von Terzi, and H.F. Fasel,** Direct numerical simulation of investigation of complete transition to turbulence via oblique breakdown at Mach 3, J. Fluid Mech., 2011, Vol. 674, P. 5–42.
11. **I.V. Egorov, V.G. Sudakov, and A.V. Fedorov,** Numerical modeling of perturbation propagation in a supersonic boundary layer, Fluid Dyn., 2004, Vol. 39, No. 6, P. 874–884.
12. **I.V. Egorov, V.G. Sudakov, and A.V. Fedorov,** Numerical modeling of the receptivity of a supersonic boundary layer to acoustic disturbances, Fluid Dyn., 2006, Vol. 41, No. 1, P. 37-48.
13. **I.V. Egorov, A.V. Fedorov, and V.G. Soudakov,** Receptivity of a hypersonic boundary layer over a flat plate with a porous coating, J. Fluid Mech., 2008, Vol. 601, P. 165–187.
14. **A. Thumm, W. Wolz, and H. Fasel,** Numerical simulation of spatially growing three-dimensional disturbance waves in compressible boundary layers, in: Laminar-Turbulent Transition, Springer, Berlin, Heidelberg, 1993, P. 303–308.
15. **C.S.J. Mayer, S. Wernz, and H.F. Fasel,** Investigation of oblique breakdown in a supersonic boundary layer, AIAA Paper, 2007, No. 2007–0940.
16. **G.S. Jiang and C.-W. Shu,** Efficient implementation of weighted ENO schemes, J. Comput. Phys., 1996, Vol. 26, P. 202–228.
17. **E. Hairer, S.P. Nørsett, and G. Wanner,** Solving Ordinary Differential Equations. I: Nonstiff Problems, Springer, Berlin, 1987.
18. **A.N. Kudryavtsev, T.V. Poplavskaya, and D.V. Khotyanovskii,** Application of higher-order schemes at the simulation of unsteady supersonic flows, Matem. Modelirovanie, 2007, Vol. 19, No. 7, P. 39–55.
19. **N.A. Adams,** Direct numerical simulation of turbulent compression ramp flow, Theor. Comp. Fluid Dyn., 1998, Vol. 12, P. 109–129.